Article:

Dhimish, Mahmoud, Holmes, Violeta, Mehrdadi, Bruce et al. (2 more authors) (2017) Output-Power Enhancement for Hot Spotted Polycrystalline Photovoltaic Solar Cells. IEEE Transactions on Device and Materials Reliability. pp. 37-45.

https://doi.org/10.1109/TDMR.2017.2780224

Output Power Enhancement for Hot Spotted Polycrystalline Photovoltaic Solar Cells

Mahmoud Dhimish, Violeta Holmes, Bruce Mehrdadi, Mark Dales, and Peter Mather

***Abstract*—Hot spotting is a reliability problem in photovoltaic (PV) panels where a mismatched cell heats up significantly and degrades PV panel output power performance. High PV cell temperature due to hot spotting can damage the cell encapsulate and lead to second breakdown, where both cause permanent damage to the PV panel. Therefore, the development of two hot spot mitigation techniques are proposed using a simple and reliable method. PV hot spots in the examined PV system was inspected using FLIR i5 thermal imaging camera.**

Multiple experiments have been tested during various environmental conditions, where the PV module I-V curve was evaluated in each observed test to analyze the output power performance before and after the activation of the proposed hot spot mitigation techniques. One PV module affected by hot spot was tested. The output power during high irradiance levels is increased by approximate to 1.26 W after the activation of the first hot spot mitigation technique. However, the second mitigation technique guarantee an increase in the power up to 3.97 W. Additional test has been examined during partial shading condition. Both proposed techniques ensure a decrease in the shaded PV cell temperature, thus an increase in the PV output power.

Index Terms— Hot spot mitigation; photovoltaic (PV) hot spotting analysis; solar cells; thermal imaging.

I. INTRODUCTION

Photovoltaic (PV) hot spots are a well-known phenomenon, described as early as in 1969 [1 and 2] and still present in PV modules [3 and 4]. PV hot spots occur when a cell, or group of cells, operates at reverse-bias, dissipating power instead of delivering it and, therefore, operating at abnormally high temperatures. This increase in the cells temperature will gradually degrade the output power generated by the PV module as explained by M. Simon & L. Meyer [5].

Hot spots are relatively frequent in current PV modules and this situation will likely persist as the PV module technology is evolving to thinner wafers, which are prone to developing micro-cracks during the manipulation process such as manufacturing, transportation, and installation [6-8].

Other reliability issues in PV modules such as PV micro cracks [9], PV module disconnection [10], maximum power point tracking (MPPT) efficiency [11], and PV wind speed and humidity variations [12]. These factors can affect the PV modules output power performance, thus decrease its annual yield energy. However, in this paper hot spots in PV modules will be investigated.

PV hot spots can be easily detected using IR inspection, which has become a common practice in current PV applications as shown in [13 and 14]. However, the impact of hot spots on operational efficiency and PV lifetime have been narrowly addressed, which helps to explain why there is lack of widely accepted procedures which deals with hot spots in practice as well as specific criteria referring to acceptance or rejection of affected PV modules in commercial frameworks as described by R. Moretón et al [15].

In the past, the increase in the number of bypass diodes (up to one diode for each cell) was proposed as a possible solution [16 and 17]. However, this approach has not encountered the favor of crystalline PV modules producers since it requires a not negligible technological cost and can be even detrimental in terms of power production when many diodes are activated because of their power consumption as discussed by S. Daliento et al [18].

In addition, the main prevention method for hot spotting is a passive bypass diode that is placed in parallel with a string of PV cells. The use of bypass diodes across PV strings is standard practice that is required in crystalline silicon PV panels [19]. Their purpose is to prevent hot spot damage that can occur in series-connected PV cells [20-22]. Bypass diodes turn "on" to provide an alternative current path and attempt to prevent extreme reverse voltage bias on PV strings. The general misunderstanding is that bypassing a string protects cells against hot spotting.

More recently, it has been shown that the distributed MPPT approach suggested by M. Coppola [23] is beneficial for mitigating the hot spot in partially shaded modules with a temperature reduction up to 20 ^{0}C for small shadows. On the other hand, authors in [24 and 25] show the "inadequateness" of the standard bypass diodes, the insertion of a series-connected switch are suited to interrupt the current flow during bypass activation process. However, this solution requires a quite complex electronic board design that needs devised power supply and appropriate control logic for activating the hot spot protection device.

This paper presents a simple solution for mitigating the impact of hot spots in PV solar cells. Two techniques are proposed, where both hot spot mitigation techniques consists of two MOSFETs connected to the PV panel which is affected by a hot spot. Several experiments have been examined during various environmental conditions. The PV module I-V curve was evaluated in each observed test to analyze the output power performance before and after the activation of the proposed hot spot mitigation techniques.

One PV module affected by a hot spot was tested. After activating the first technique the output power of the PV module increased by 1.26 W in high irradiance levels, 1.44 W in medium irradiance levels and 0.48 W in low irradiance levels. Same experiments were carried out using the 2nd proposed hot spot mitigation technique, while the

Mahmoud Dhimish, Violeta Holmes, Bruce Mehrdadi, Mark Dales and Peter Mather are with the Department of Engineering and Technology, University of Huddersfield, HD1 3DH, UK (email: Mahmoud.dhimish2@hud.ac.uk; V.Holmes@hud.ac.uk; B.R.Mehrdadi@hud.ac.uk, m.r.dales@hud.ac.uk, p.mather@hud.ac.uk).

output power increased by 3.97 W for high irradiance levels, 3.51 W in medium irradiance levels and 1.31 W in low irradiance levels.

This paper is organized as follows: section II presents the examined PV module electrical characteristics, while section III describes the proposed hot spot mitigation techniques. Section IV shows the validation process of the proposed hot spot protection method using two case studies. Lastly, section V demonstrates the conclusion and the future work.

II. EXAMINED PHOTOVOLTAIC MODULE CHARACTERISTICS

In this work, the PV system used comprises a PV plant containing 9 polycrystalline silicon PV modules each with a nominal power of 220 W_p. The photovoltaic modules are organized in 3 strings and each string is made up of 3 series-connected PV modules. Using a photovoltaic connection unit which is used to enable or disable the connection for any PV module from the entire PV plant. Each photovoltaic string is connected to a Maximum Power Point Tracker (MPPT) unit which has an output efficiency not less than 98.5% [26]. The existing PV system is shown in Fig. 1.

The SMT6 (60) P solar module manufactured by Romag has been used. The tilt angle of the PV installation is 42°. The electrical characteristics of the solar modules are shown in Table 1. Additionally, the standard test condition (STC) for these solar panels are: solar irradiance (G): 1000 W/m^2 and module temperature (T): 25 °C.

Fig. 1. Examined PV system installed at the University of Huddersfield, United Kingdom

TABLE I
PV MODULE ELECTRICAL CHARACTERISTICS

PV module parameter	Value
PV peak power	220 W
One PV cell peak power	3.6 W
Voltage at maximum power point (V_{mpp})	28.7 V
Current at maximum power point (Impp)	7.67 A
Open Circuit Voltage (V_{oc})	36.74 V
Short Circuit Current (I_{sc})	8.24 A
Number of cells connected in series	60
Number of cells connected in parallel	1

III. HOT SPOT DETECTION AND PROTECTION SYSTEM

The investigation of the hot spots in the tested PV system was captured using i5 FLIR thermal camera as shown in Fig. 2, where its specification is shown in Table 2 [27]. After examining the hot spots in the PV modules, the hot spot mitigation techniques will be activated.

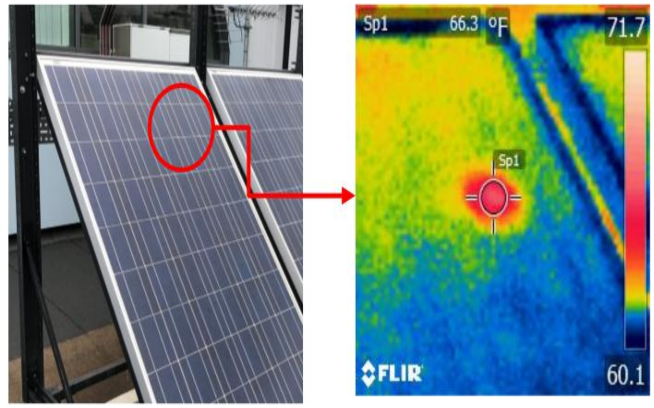

Fig. 2. Hot Spot detection using FLIR thermal camera

TABLE 2
FLIR I5 CAMERA SPECIFICATION

Comparison	Value
Thermal image quality	100x100 pixels
Field of view	21^0 (H) x 21^0 (V)
Thermal sensitivity	32.18 F

The first proposed hot spot protection system is connected to each PV string in the PV module. As can be seen in Fig. 3(a), the examined PV module used in this work contains three sub strings connected throw bypass diodes. In order to apply the proposed hot spot mitigation technique, two MOSFETs were connected to each PV string as shown in Fig. 3(b). Switch 1 is in series with the PV string and is normally "on"; it opens when a hot spot condition is detected to prevent further hot spotting. While, switch 2 is in parallel with the PV string and it is normally in "open" mode, it turns "on" to allow a bypass current path when the PV string is open circuited.

Another hot spot mitigation technique was used with the PV module instead of the connection for each MOSFET to the PV string as shown in Fig. 3(c). The same concept has been applied, where switch 1 is in series with the PV module is normally "on"; it opens when a hot spot condition is detected to prevent further hot spotting. Switch 2 is in parallel with the PV module and is normally "open"; it turn "on" to allow a bypass current path when the PV string is open circuited. The two switch PV protection device has been implemented and connected to the PV panel which contains the hot spot.

As can be noticed, the proposed techniques are simple to implement, where the connection steps is also within the PV module limit, since it requires only to add additional MOSFETs to the hot spotted PV module. In the next section, the validation and comparison between the developed hot spot mitigation techniques will be presented.

IV. VALIDATION OF THE PROPOSED HOT SPOT MITIGATION TECHNIQUES

In this section the validation for both proposed hot spot mitigation techniques are illustrated and compared in brief. The output power are compared using the I-V curve analysis, and the detection of the hot spots have been captured using i5 FLIR camera.

A. *PV Hot Spot and I-V Curve Analysis*

The proposed hot spotting techniques were tested in an experimental setup with a resistive load powered by the PV module which contains the hot spot previously shown in Fig. 2. The MOSFETs are placed in the examined PV module as shown in Fig. 3(b) and Fig. 3(c).

There are several stages that have been carried out during the operation of the proposed hot spotting mitigation techniques, these stages are describes as follows:

i. **Hot spot mitigation technique 1:**

The results obtained by the first mitigation technique is shown in Fig. 4(a), the results can be described as the following:

a) Before the activation: the temperature of the hot spotted PV solar cell is equal to 70 ^{0}F, while the adjacent (reference) solar cells temperature is equal to 61.5 ^{0}F.
b) 1 minute after the activation: the temperature of the hot spotted PV solar cell reduced to 68.7 ^{0}F, the difference between the hot spotted PV solar cell with the reference solar cell temperature is equal to 7.2 ^{0}F.
c) 2 minutes after the activation: the maximum enhancement of the temperature for the hot spotted PV solar cell is reduced to 67.1 ^{0}F, comparing to 70 ^{0}F before the activation of the mitigation technique.

ii. **Hot spot mitigation technique 2:**

The results obtained by the first mitigation technique is shown in Fig. 4(b), the results can be described as the following:

a) Before the activation: the temperature of the hot spotted PV solar cell is equal to 70.6 ^{0}F, while the adjacent (reference) solar cells temperature is equal to 61.8 ^{0}F.
b) 1 minute after the activation: the temperature of the hot spotted PV solar cell reduced to 66.3 ^{0}F, the difference between the hot spotted PV solar cell with the reference solar cell temperature is equal to 4.5 ^{0}F.
c) 2 minutes after the activation: the maximum enhancement of the temperature for the hot spotted PV solar cell is reduced to 64.9 ^{0}F, comparing to 70.6 ^{0}F before the activation of the mitigation technique.

As can be noticed, the obtained results from the hot spot mitigation technique 2 has better performance comparing to technique 1, where the where the maximum difference between the hot spotted PV solar cell and the adjacent solar cells is equal to 3.1 ^{0}F.

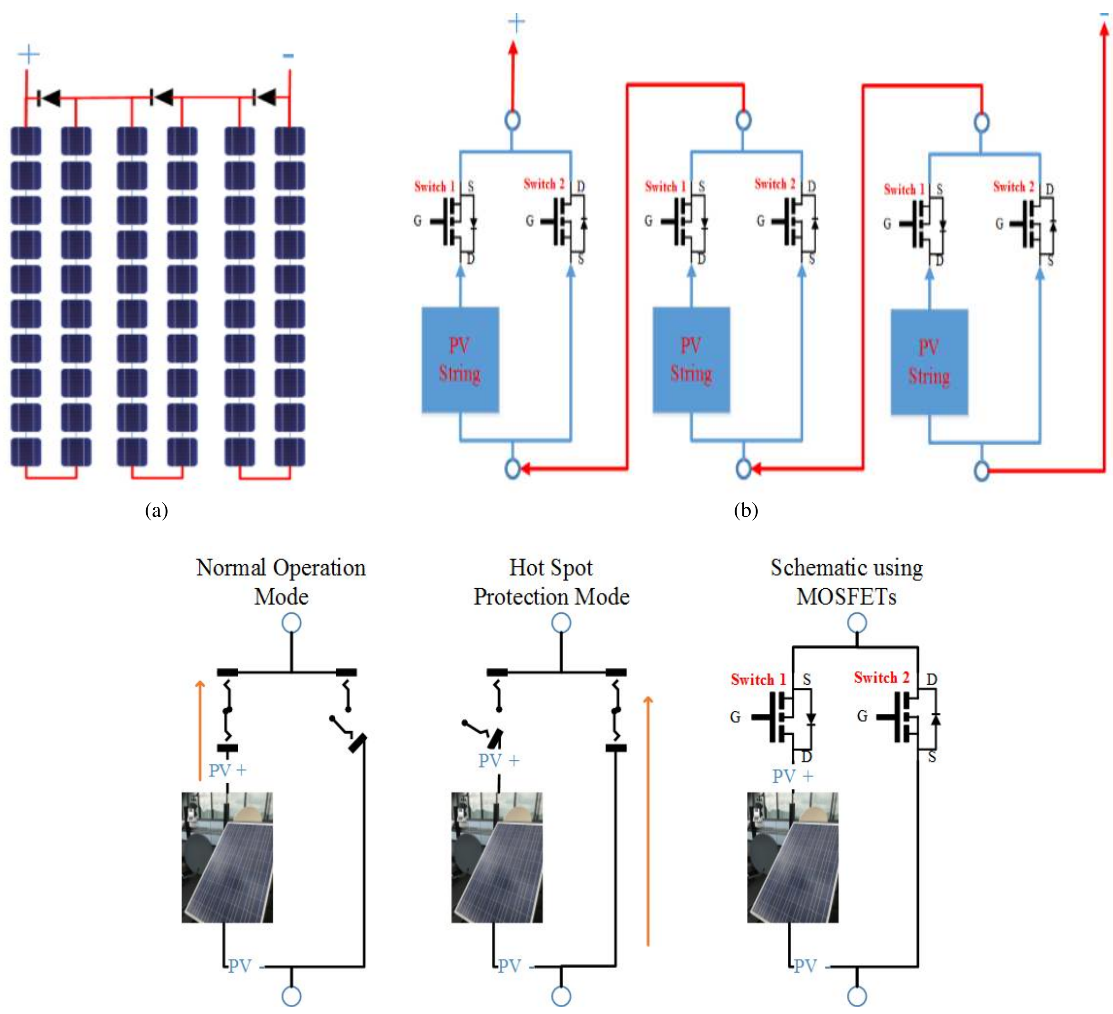

Fig. 3. (a) Structure of the PV string in the examined PV module, (b) First hot spot mitigation technique, (c) Second proposed hot spot mitigation technique

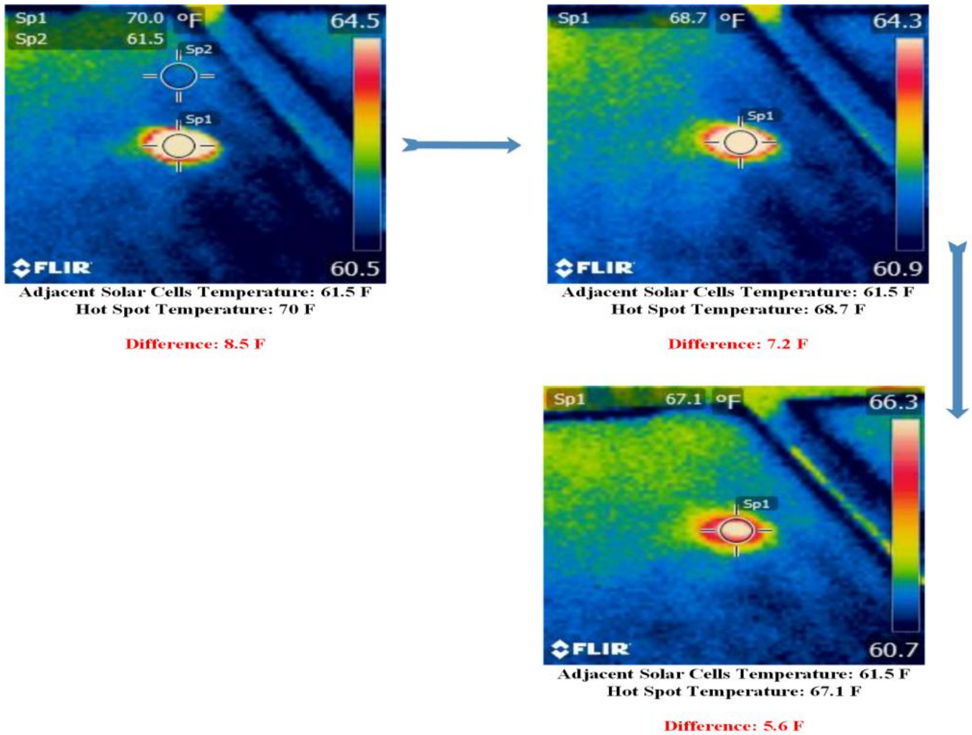

(a)

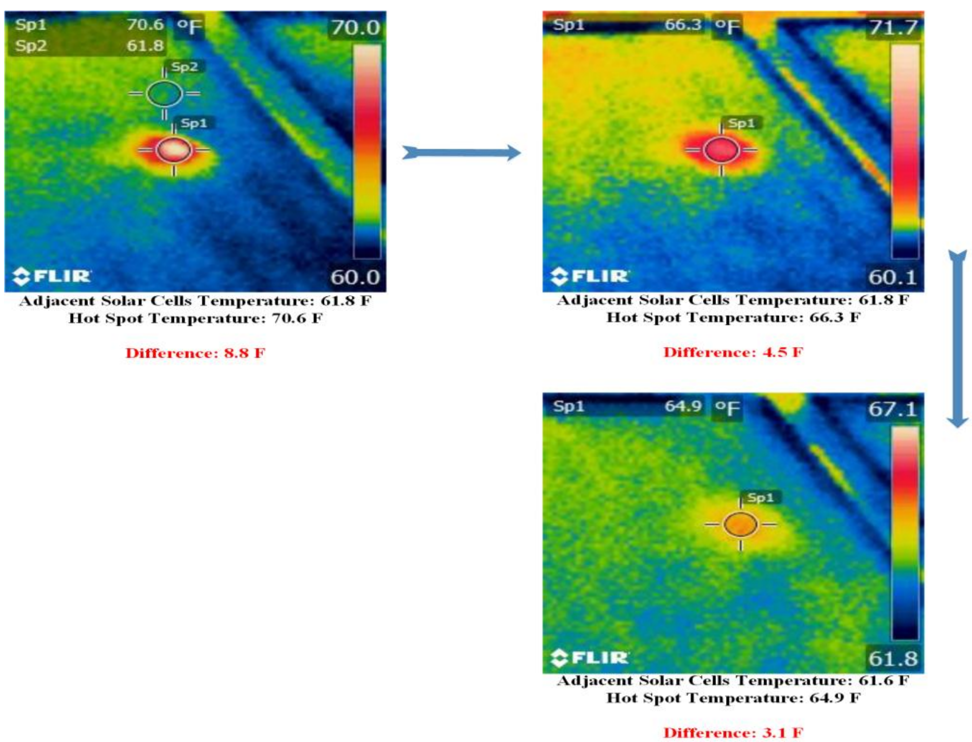

(b)

Fig. 4. (a) Output hot spot mitigation using technique 1, (b) Output hot spot mitigation using technique 2

The main reason for the proposed hot spotting mitigation technique is to improve the output power efficiency for the examined hot spotted PV modules.

The value of the power before and after the activation for each proposed technique was monitored in three different irradiance levels: High irradiance level: 840 W/m^2, medium irradiance level: 507 W/m^2 and low irradiance level: 177 W/m^2, while in all tested scenarios, the PV temperature is estimated at a fixed value approximately equals to 16.2 ^{o}C.

Fig. 5(a) shows the output I-V curves of the PV module at high irradiance level. The measured output power after the activation of the proposed 1st technique has a power loss equals to 3.95 W comparing to 5.21 W with no mitigation technique deployed in the PV module. However, the minimum loss in the output power is estimated while activating the 2nd hot spotted mitigation technique (P_{loss} = 1.24 W). A brief comparison between both examined techniques are shown in Table 3.

The output I-V curves for the examined PV module under medium and low irradiance levels are shown in Fig. 5(b) and Fig. 5(c) respectively. The output results show a significant improvement in the output power while activating the 2nd hot spot mitigation technique comparing to the 1st technique. Table 3 shows a comparison of the output results in each examined irradiance level.

In conclusion, this section shows the validation and the enhancement in the PV temperature and the output power generated by the PV module using both proposed hot spot mitigation techniques. Technique 2 has a better performance comparing to the 1st proposed mitigation technique in both, PV output power and the maximum reduction in the hot spotted solar cell temperature.

Moreover, Power MOSFETs IRFZ44V were used to implement and test the suggested hot spot mitigation techniques. The MOSFETs drain-to-source breakdown voltage is equal to 60 V, and the voltage drop in drain-to-source as low as 50 mV. The cost of the MOSFET is equal to £0.85. Therefore, the total cost for the first and second presented techniques using one PV module are equal to £5.1 and £1.7 respectively.

There are no electrical complexity in developing both mitigation techniques as a commercial product, since it is only require to add the MOSFETs in series with the hot spotted PV module.

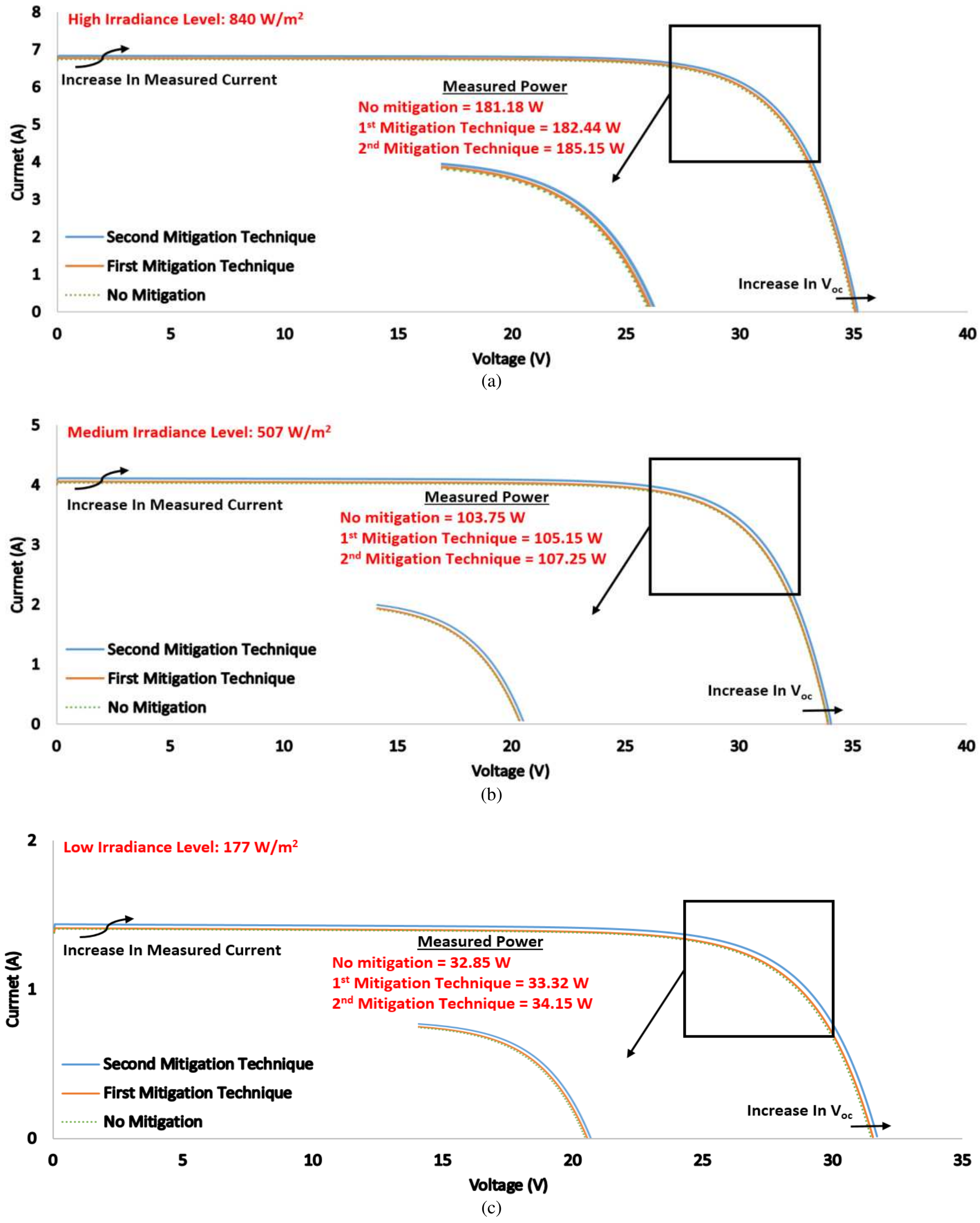

Fig. 5. Photovoltaic I-V curve. (a) Before and after considering hot spot mitigation techniques at G: 840 W/m², (b) Before and after considering hot spot mitigation techniques at G: 507 W/m², (c) Before and after considering hot spot mitigation techniques at G: 177 W/m²

TABLE 3

COMPARISON BETWEEN THE FIRST AND SECOND PROPOSED HOT SPOT MITIGATION TECHNIQUE USING HIGH, MEDIUM AND LOW IRRADIANCE LEVELS

Irradiance (W/m^2)	Theoretical Power (W)	Case Scenario	Voltage (V)	Current (A)	Power (W)	P_{loss} (W)	Efficiency (%)
High 840	186.4	No mitigation	28.59	6.33	181.18	5.21	97.2
		1st Technique	28.67	6.36	182.44	3.95	97.88
		2nd Technique	28.93	6.40	185.15	1.24	99.33
Medium 507	108.2	No mitigation	27.31	3.79	103.75	4.45	95.89
		1st Technique	27.39	3.83	105.15	3.01	97.18
		2nd Technique	27.69	3.87	107.25	0.94	99.12
Low 177	34.4	No mitigation	25.27	1.30	32.85	1.55	95.51
		1st Technique	25.44	1.31	33.33	1.07	96.88
		2nd Technique	25.68	1.33	34.15	0.24	99.28

B. *Partial Shading Analysis*

The main purpose of this section is to test the ability of the proposed hot spot mitigation techniques to increase the output power of the PV module in partial shading conditions affecting any PV module; it is not necessary that the tested PV module has a hot spotted PV solar cell.

In order to test the ability of the proposed hot spot mitigation technique, another experimental setup has been tested on a PV module with partially shaded solar cell. Fig. 6 shows an image for the examined PV module under shaded solar cell using paper opaque object. The PV module was examined at irradiance level of 784 W/m^2. The temperature of the shaded solar cell was captured using the i5 FLIR camera.

The first test was carried out using the activation of the first proposed hot spot mitigation technique. Fig. 7(a) shows the thermography image of the shaded solar cell before and after the activation of the 1st mitigation technique.

Fig. 6. Opaque paper object covering one solar cell

Before the activation, the temperature of the shaded solar cell is equal to 66.6 ^{0}F. The solar cell temperature decreases to a minimum value of 63.9 ^{0}F after the activation of the hot spot mitigation technique.

This decrease in the value of the temperature will guarantee an increase in the output power produced by the PV module. As illustrated in Fig. 8(a), the output power before and after the activation is equal to 171.787 W and 172.508 W respectively. Thus, the total increase in the output power is equal to 0.721 W.

The second test was carried out using the activating of the second proposed hot spot mitigation technique. Fig. 7(b) displays the thermography images of the examined shaded solar cell before and after activating the mitigation technique.

The difference in the temperature of the shaded solar cell is shown in (1).

Difference = (No mitigation) 71.0 ^{0}F – (After activating the 2nd hot spot mitigation technique) 65.3 F = 5.7 ^{0}F (1)

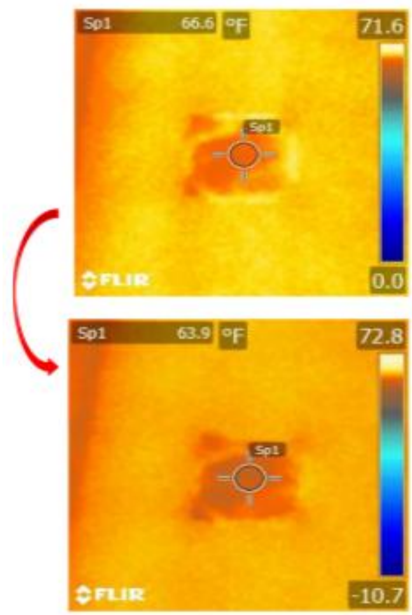

(a)

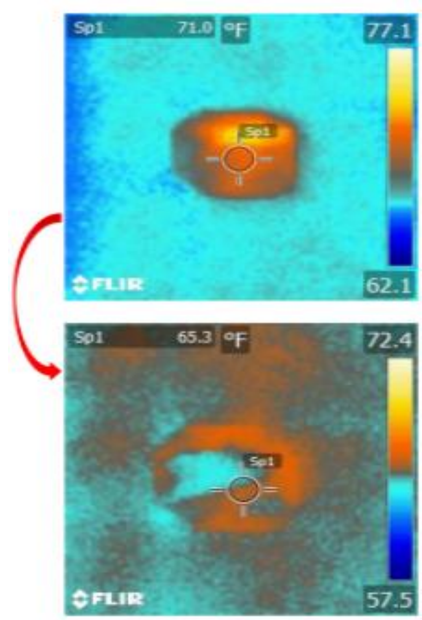

(b)

Fig. 7. (a) Thermographic image of the shaded PV solar cell before and after the activation of the first hot spot mitigation technique, (b) Thermographic image of the shaded PV solar cell before and after the activation of the second hot spot mitigation technique

This decrease in the temperature of the shaded solar cell guarantee an increase in the measured maximum power point of the PV module. Fig. 8(b) shows that the total increase in the measured output power which is equal to 1.689 W.

In conclusion, this section demonstrates that both proposed hot spot mitigation techniques are useful in case a partial shading conditions occurs in the PV module. An enhancement of the temperature and output power of the PV module is guaranteed. In addition, the second proposed hot spot mitigation technique shows better performance comparing to the 1st technique.

V. Conclusion

In this paper, the design and development for two hot spot mitigation techniques are proposed. The offered techniques are capable to enhance the output power of PV modules which are effected by hot spots and partial shading conditions. Both techniques use two MOSFTEs in the affected PV module. Several experiments have been examined during various environmental conditions, where the PV module I-V curve was evaluated in each observed test to analyze the output power performance before and after the activation of both proposed hot spot mitigation techniques. One PV module affected by a hot spot was tested. After activating the first mitigation technique the output power of the PV module increased by 1.26 W in high irradiance levels, 1.44 W in medium irradiance level and 0.48 W in low irradiance level. Same experiments were carried out using the 2nd proposed hot spot mitigation technique, while the output power increased by 3.97 W for high irradiance levels, 3.51 in medium irradiance levels and 1.31 W in low irradiance levels.

References

[1] Blake, F. A., & Hanson, K. L. (1969, August). The hot-spot failure mode for solar arrays. In *Proceedings of the 4th Intersociety Energy Conversion Engineering Conference* (pp. 575-581).

[2] Carrasco, J. M., Franquelo, L. G., Bialasiewicz, J. T., Galván, E., PortilloGuisado, R. C., Prats, M. M., ... & Moreno-Alfonso, N. (2006). Power-electronic systems for the grid integration of renewable energy sources: A survey. *IEEE Transactions on industrial electronics*, *53*(4), 1002-1016.

[3] Dhimish, M., Holmes, V., Mehrdadi, B., Dales, M., Chong, B., & Zhang, L. (2017). Seven indicators variations for multiple PV array configurations under partial shading and faulty PV conditions. *Renewable Energy*.

[4] Orduz, R., Solórzano, J., Egido, M. Á., & Román, E. (2013). Analytical study and evaluation results of power optimizers for distributed power conditioning in photovoltaic arrays. *Progress in Photovoltaics: Research and Applications*, *21*(3), 359-373.

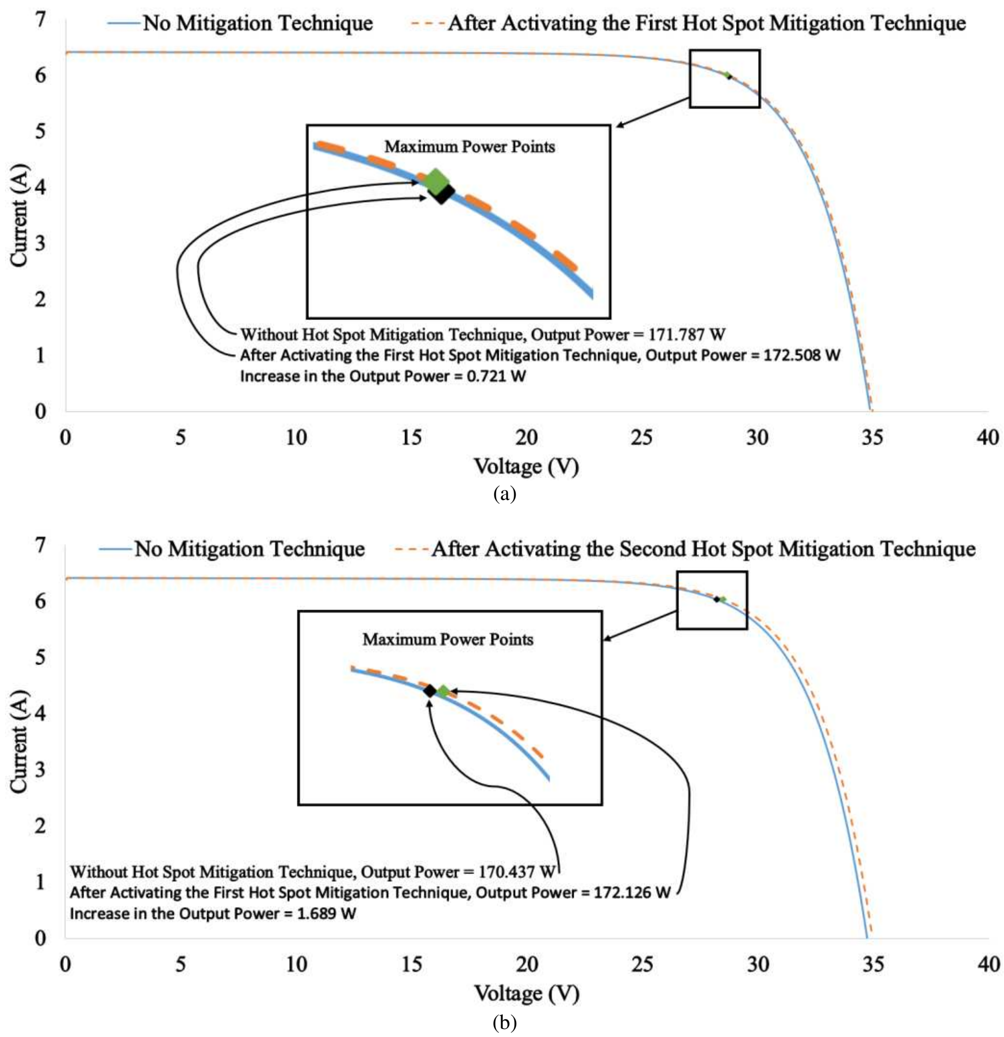

Fig. 8. Photovoltaic output I-V curve. (a) Before and after activating the first hot spot mitigation technique, (b) before and after activating the second hot spot mitigation technique

[5] Simon, M., & Meyer, E. L. (2010). Detection and analysis of hot-spot formation in solar cells. *Solar Energy Materials and Solar Cells*, *94*(2), 106-113.
[6] Hu, Y., Cao, W., Ma, J., Finney, S. J., & Li, D. (2014). Identifying PV module mismatch faults by a thermography-based temperature distribution analysis. *IEEE Transactions on Device and Materials Reliability*, *14*(4), 951-960.
[7] Chaturvedi, P., Hoex, B., & Walsh, T. M. (2013). Broken metal fingers in silicon wafer solar cells and PV modules. *Solar Energy Materials and Solar Cells*, *108*, 78-81.
[8] M. Dhimish, V. Holmes, B. Mehrdadi, M. Dales, The Impact of Cracks on Photovoltaic Power Performance, *Journal of Science: Advanced Materials and Devices* (2017), doi: 10.1016/j.jsamd.2017.05.005.
[9] Dhimish, M., Holmes, V., Dales, M., & Mehrdadi, B. (2017). The effect of micro cracks on photovoltaic output power: case study based on real time long term data measurements. *Micro & Nano Letters*.
[10] Dhimish, M., Holmes, V., Mehrdadi, B., & Dales, M. (2017). Simultaneous fault detection algorithm for grid-connected photovoltaic plants. *IET Renewable Power Generation*.
[11] Chen, S. H., Huang, T. C., Ng, S. S., Lin, K. L., Du, M. J., Kang, Y. C., ... & Lin, J. R. (2016). A Direct AC–DC and DC–DC Cross-Source Energy Harvesting Circuit with Analog Iterating-Based MPPT Technique with 72.5% Conversion Efficiency and 94.6% Tracking Efficiency. *IEEE Transactions on Power Electronics*, *31*(8), 5885-5899.
[12] Mekhilef, S., Saidur, R., & Kamalisarvestani, M. (2012). Effect of dust, humidity and air velocity on efficiency of photovoltaic cells. *Renewable and Sustainable Energy Reviews*, *16*(5), 2920-2925.
[13] Buerhop, C., Schlegel, D., Niess, M., Vodermayer, C., Weißmann, R., & Brabec, C. J. (2012). Reliability of IR-imaging of PV-plants under operating conditions. *Solar Energy Materials and Solar Cells*, *107*, 154-164.
[14] Solórzano, J., & Egido, M. A. (2014). Hot-spot mitigation in PV arrays with distributed MPPT (DMPPT). *Solar Energy*, *101*, 131-137.
[15] Moretón, R., Lorenzo, E., & Narvarte, L. (2015). Experimental observations on hot-spots and derived acceptance/rejection criteria. *Solar energy*, *118*, 28-40.
[16] Hasyim, E. S., Wenham, S. R., & Green, M. A. (1986). Shadow tolerance of modules incorporating integral bypass diode solar cells. *Solar cells*, *19*(2), 109-122.
[17] Chen, K., Chen, D., Zhu, Y., & Shen, H. (2012). Study of crystalline silicon solar cells with integrated bypass diodes. *Science China Technological Sciences*, *55*(3), 594-599.
[18] Daliento, S., Mele, L., Bobeico, E., Lancellotti, L., & Morvillo, P. (2007). Analytical modelling and minority current measurements for the determination of the emitter surface recombination velocity in silicon solar cells. *Solar energy materials and solar cells*, *91*(8), 707-713.
[19] García, M., Marroyo, L., Lorenzo, E., Marcos, J., & Pérez, M. (2014). Observed degradation in photovoltaic plants affected by hot-spots. *Progress in Photovoltaics: Research and applications*, *22*(12), 1292-1301.
[20] Dhimish, M., & Holmes, V. (2016). Fault detection algorithm for grid-connected photovoltaic plants. *Solar Energy*, *137*, 236-245.
[21] Silvestre, S., Boronat, A., & Chouder, A. (2009). Study of bypass diodes configuration on PV modules. *Applied Energy*, *86*(9), 1632-1640.
[22] Dhimish, M., Holmes, V., Mehrdadi, B., & Dales, M. (2017). Diagnostic method for photovoltaic systems based on six layer detection algorithm. *Electric Power Systems Research*, *151*, 26-39.
[23] Coppola, M., Daliento, S., Guerriero, P., Lauria, D., & Napoli, E. (2012, June). On the design and the control of a coupled-inductors boost dc-ac converter for an individual PV panel. In *Power Electronics, Electrical Drives, Automation and Motion (SPEEDAM), 2012 International Symposium on* (pp. 1154-1159). IEEE.
[24] Kim, K. A., & Krein, P. T. (2015). Reexamination of photovoltaic hot spotting to show inadequacy of the bypass diode. *IEEE Journal of Photovoltaics*, *5*(5), 1435-1441.
[25] d'Alessandro, V., Guerriero, P., Daliento, S., & Gargiulo, M. (2011). A straightforward method to extract the shunt resistance of photovoltaic cells from current–voltage characteristics of mounted arrays. *Solid-State Electronics*, *63*(1), 130-136.
[26] M. Dhimish, V. Holmes, M. Dales, Parallel fault detection algorithm for grid-connected photovoltaic plants, Renewable Energy (2017), doi: 10.1016/j.renene.2017.05.084.
[27] Dhimish, M., Holmes, V., Mehrdadi, B., Dales, M., & Mather, P. (2017). Photovoltaic fault detection algorithm based on theoretical curves modelling and fuzzy classification system. *Energy*.

Mahmoud Dhimish received his M.Sc. degree in electrical and communication engineering from the University of Huddersfield, United Kingdom, in 2015, where he is currently working toward the Ph.D. degree in renewable energy systems. His research interest include design, control and performance analysis of photovoltaic power conditioning systems using novel mathematical modelling techniques.

Violeta Holmes is a Subject Area Leader for Electronic and Electrical Engineering at the Huddersfield University with over 25 years of teaching and research experience in computing and engineering. She leads the High Performance Computing (HPC) Research Group at the University of Huddersfield. Her research interests and expertise are in the areas of HPC systems infrastructure, Internet of Things and Embedded Systems.

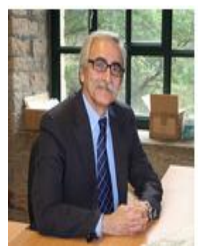

Bruce Mehrdadi is an MSc engineering programme leader and international recruitment manager for engineering courses at School of Computing and Engineering, University of Huddersfield. His main teaching area in in Embedded Systems and Computer interacting. His research interests and expertise are in the areas of Embedded Systems, Internet of Things and Renewable energy systems.

Mark Dales is an Electrical Engineer and prior to becoming a University Lecturer in 2003, he spent 30 years working in the Electricity Supply Industry (ESI). Following his initial education and training, he was employed in the 'Meters, Testing and Protection ' section. His responsibilities included testing, commissioning and carrying out fault diagnoses on industrial metering schemes, power system protection equipment and telecommunications systems.

Peter Mather is a senior lecturer at School of Computing and Engineering, University of Huddersfield. He is the course leader for all the MEng/BEng & BSc electronics courses. He is currently developing a wide range of electronic and associated systems from VHDL/FPGA development to Sigma-Delta ADC testing of mixed signal devices. He also investigating integrated sustainable energy networks in order to optimize commercial and domestic energy usage within existing premises.